Published in final edited form as:
Biochim Biophys Acta. 2013 February ; 1828(2): 398–404. doi:10.1016/j.bbamem.2012.09.014.

NMR resolved multiple anesthetic binding sites in the TM domains of the α4β2 nAChR

Vasyl Bondarenko[1,*], **David Mowrey**[1,3,*], **Lu Tian Liu**[1], **Yan Xu**[1,2,4], and **Pei Tang**[1,3,4]

[1]Department of Anesthesiology, University of Pittsburgh School of Medicine

[2]Department of Structural Biology, University of Pittsburgh School of Medicine

[3]Department of Computational & Systems Biology, University of Pittsburgh School of Medicine

[4]Department of Pharmacology & Chemical Biology, University of Pittsburgh School of Medicine

Abstract

The α4β2 nicotinic acetylcholine receptor (nAChR) has significant roles in nervous system function and disease. It is also a molecular target of general anesthetics. Anesthetics inhibit the α4β2 nAChR at clinically relevant concentrations, but their binding sites in α4β2 remain unclear. The recently determined NMR structures of the α4β2 nAChR transmembrane (TM) domains provide valuable frameworks for identifying the binding sites. In this study, we performed solution NMR experiments on the α4β2 TM domains in the absence and presence of halothane and ketamine. Both anesthetics were found in an intra-subunit cavity near the extracellular end of the 2 transmembrane helices, homologous to a common anesthetic binding site observed in X-ray structures of anesthetic-bound GLIC (Nury, et. al. 2011). Halothane, but not ketamine, was also found in cavities adjacent to the common anesthetic site at the interface of α4 and β2. In addition, both anesthetics bound to cavities near the ion selectivity filter at the intracellular end of the TM domains. Anesthetic binding induced profound changes in protein conformational exchanges. A number of residues, close to or remote from the binding sites, showed resonance signal splitting from single to double peaks, signifying that anesthetics decreased conformation exchange rates. It was also evident that anesthetics shifted population of two conformations. Altogether, the study comprehensively resolved anesthetic binding sites in the α4β2 nAChR. Furthermore, the study provided compelling experimental evidence of anesthetic-induced changes in protein dynamics, especially near regions of the hydrophobic gate and ion selectivity filter that directly regulate channel functions.

Keywords

halothane; ketamine; general anesthetics; NMR; α4β2 nAChR; protein dynamics

Send all correspondence to: Professor Pei Tang, Ph.D., 2049 Biomedical Science Tower 3, 3501 Fifth Avenue, University of Pittsburgh, Pittsburgh, Pennsylvania 15260, Tel (412) 383–9798, Fax (412) 648-8998, tangp@upmc.edu.
*Both authors contributed equally to the work

Introduction

Although general anesthesia has been used clinically for over a century, the molecular mechanism is still under investigation. Cys-loop receptors, including nicotinic acetylcholine receptors (nAChRs), are the important targets of general anesthetics [1, 2]. Among many different subtypes of nAChRs, the α4β2 nAChR is one of the most abundant nAChRs in the brain [3]. It is involved in memory [4], nociception [5], and autonomic response [6]. It is highly sensitive to a variety of general anesthetics. Its current is inhibited by both volatile and intravenous general anesthetics at clinically relevant concentrations [7–9]. The α4β2 nAChR shares the same structural architecture as other members of the Cys-loop superfamily. It forms a pentameric ligand-gated ion channel with alternating α4 and β2 subunits arranged around the channel axis in the 3:2 or 2:3 molar ratio [10, 11]. Each subunit has an extracellular (EC) domain and a transmembrane (TM) domain, which contains four membrane-spanning helices (TM1-TM4) with TM2 lining the channel pore. The intracellular (IC) domain contains a large linker between TM3 and TM4. Dissecting anesthetic action on the α4β2 nAChR will offer valuable insights into the mechanism of anesthetic modulation on Cys-loop receptors.

To reveal the underlying mechanism of anesthetic inhibition of a channel protein, an essential task is to identify where anesthetics bind to the protein. Mutagenesis has been widely used to determine residues showing different functional responses to anesthetics before and after mutations [12–14]. Such an approach is useful, but it is difficult to differentiate direct binding from allosteric action. Photoaffinity labeling has emerged as a powerful tool for identifying specific protein residues participating in anesthetic binding [1, 15–20]. Analogues of halothane [19], etomidate [18, 21, 22], and a neurosteroid [16] were photolabeled onto the *Torpedo* nAChR or the $GABA_A$ receptors. Multiple binding sites were identified in the TM domains and other regions of the receptors. Despite considerable progress in developing new anesthetic analogues for photolabeling [23–25], the choices of anesthetics for photolabeling are still limited. In addition, large hydrophobic patches within the TM domain often hinder amino acid sequencing and have made it difficult to determine specific photolabeled residues in some channel proteins. X-ray crystallography can offer high-resolution structural information for anesthetic binding. A critical issue is whether a good quality crystal is attainable for the selected protein. Structural determination of eukaryotic Cys-loop receptors remains a great challenge, but recent successes on structures of the prokaryotic homologues are certainly encouraging [26–29]. Crystal structures of the ligand-bound ELIC [30, 31], especially structural elucidation of anesthetic desflurane or propofol binding to the TM domain of GLIC [32], shed light on molecular recognition of general anesthetics in Cys-loop receptors. Nuclear magnetic resonance (NMR) spectroscopy is yet another powerful technique for structural determinations of ion channels [33–36] and probing protein-ligand interactions at the atomic level. Using NMR, we have identified specific sites of anesthetic interaction with the TM domains of several proteins [37–43]. Furthermore, NMR could resolve site-specific changes in protein dynamics introduced by anesthetics [37–39] that are indispensable for understanding functional impact of anesthetic binding.

In this study, we used NMR spectroscopy to examine the plausible binding sites of the volatile anesthetic halothane and the intravenous anesthetic ketamine within the TM domains of the α4β2 nAChR. We previously determined the structures of the entire TM domains of the α4 (PDB ID: 2LLY) and β2 (PDB ID: 2LM2) nAChRs in LDAO detergent micelles by solution NMR [35]. We demonstrated that the TM domains of α4 and β2 could assemble into a pentameric pore-forming structure [35]. We also demonstrated that the assemblies of the TM domains or even the TM2 helices of α4 and β2 conduct Na^+ [35, 37]. The high-resolution structure of the α4β2 TM domain provides an excellent platform for

investigating anesthetic binding sites as well as protein dynamics changes that may be responsible for anesthetic inhibition of the α4β2 nAChR. The knowledge of anesthetic binding sites combined with the dynamic impact on the TM domains is essential for solving the mystery of anesthetic modulations of the α4β2 nAChR as well as other Cys-loop receptors.

2. Materials and Methods

2.1 Sample Preparations

Expression and purification of the α4 and β2 TM domains of the human nAChR as well as the NMR sample preparation were reported in detail recently [35]. The same protein expression and purification protocols were used for the current study. Each NMR sample contained 0.25–0.3 mM protein, 1–2 % (40–80 mM) LDAO detergent, 5 mM sodium acetate pH 4.7, 10 mM NaCl, and 20 mM 2-mercaptoethanol to prevent disulfide bond formation. 5% D_2O was added to the samples for deuterium lock in NMR measurements. To keep adequate NMR spectral resolution, two types of the NMR samples were prepared for investigating anesthetic binding and the associated dynamic changes. One is β2(α4), in which β2 is ^{15}N-labeled (NMR observable) and mixed with the unlabeled α4 (invisible in ^{15}N NMR) in a 3:2 molar ratio. Another type is α4(β2) that has α4 ^{15}N-labeled and mixed with unlabeled β2 in a 3:2 molar ratio. In these individually labeled α4β2 samples, α4 and β2 retained their assembling interfaces and gained better NMR spectral resolution. The anesthetic ketamine or halothane were titrated to the samples using a micropipette or a gas-tight microsyringe, respectively. The ketamine concentration in the NMR samples was calculated based on the concentration of a stock solution. The halothane concentration was quantified based on ^{19}F NMR using the method reported previously [42].

2.2 NMR data acquisition, processing, and analysis

NMR spectra were acquired on Bruker Avance 600, 700, or 800 MHz spectrometers at 45 °C. Each spectrometer was equipped with a triple-resonance inverse-detection cryoprobe, TCI (Bruker Instruments, Billerica, MA). ^{1}H-^{15}N TROSY-HSQC spectra were acquired for each sample before and after ading anesthetics. Concentrations of halothane and ketamined used for the NMR experiments were up to 8 and 0.3 mM, respectively. Spectral windows of 13 ppm (1024 data points) in the ^{1}H dimension and 22 or 24 ppm (128 data points) in ^{15}N dimension were used. One second relaxation delay was used. The specific α4 and β2 residues affected by anesthetic binding were identified based on chemical shift changes induced by anesthetics. Since halothane has a distinct proton resonance that is suitable for saturation transfer used to determine halothane binding sites, we also performed 2D saturation transfer experiments using a modified HSQC pulse sequence [39] on the β2(α4) and α4(β2) samples containing ~2.0 mM halothane that has a distinct proton resonance. The spectra were acquired in an interleaved fashion with on- and off-^{1}H resonance frequencies of 6.48 ppm (the halothane proton) and 15 ppm (blank), respectively. The selective saturation was achieved using an IBURP2 pulse train (50 ms Gaus1.1000-shaped or rectangular pulses with an interpulse delay of 4 μs). A total saturation time was one sec and a relaxation delay was 1.5 sec. The 1D saturation transfer difference experiments [44] were performed to confirm that the saturation parameters used in 2D experiments were chosen properly. The ^{1}H chemical shifts were referenced to the DSS resonance at 0 ppm and the ^{15}N chemical shifts were indirectly referenced [45].

NMR data were processed using NMRPipe 4.1 and NMRDraw 1.8 [46], and analyzed using Sparky 3.10 [47]. Each processed spectrum had 4096 × 512 data points. ^{1}H and ^{15}N chemical shift assignments for the α4 and β2 TM domains after addtion of anesthetics were referenced to the previous assignments for the same proteins without drugs [35]. The

published pentameric models of α4β2 and the MATLAB® programming environment were used to analyze interactions between anesthetics and α4β2. Chemical shifts and peak intensities in the NMR spectra were measured using Sparky 3.10 [47].

2.3 Visualization of anesthetics in the α4β2 nAChR

To assist visualizing anesthetics in the NMR identified binding sites, we performed targeted docking of halothane or ketamine to our previously reported α4β2 model. The targeted docking kept only those sites consistent with the NMR results. Docking was performed with Autodock4 [48] using a Lamarckian genetic algorithm with a grid spacing of 0.402 Å. For each intra-subunit site suggested by the NMR data, 250 independent anesthetic dockings were performed within a cube covering ~9000 $Å^3$ located at either the EC or IC end of the TM domain. For each inter-subunit site, 500 independent anesthetic dockings were performed within a ~21× 21 x 42 Å rectangular prism covering the length of the inter-subunit interface.

3. Results

3.1 Multiple halothane interaction sites in the α4β2 nAChR

Halothane bound to inter- and intra-subunit cavities of the α4β2 TM domains. As exhibited in the ^{1}H-^{15}N HSQC spectra in Fig. 1, the majority of residues were not affected when 2mM halothane was added to either the α4(β2) or the β2(α4) samples. However, some residues had obvious changes in chemical shift. Full assignments of the NMR spectra showing halothane effects are provided in Figs. S1 and S2. Direct interactions between halothane and α4β2 were further demonstrated in 2D saturation transfer experiments [49, 50] (Fig. S3). After the residues showing changes either in chemical shift or saturation transfer were mapped onto the structure of α4β2 (Fig. 2), the halothane interaction sites became apparent. The β2 subunit has two intra-subunit halothane binding sites near the EC and IC ends of the TM domain. The closeness of hydrogen atoms of halothane to Y212 and V262 (site #1 in Fig. 2) and to T224 and F231 (site #2) facilitated the observed saturation transfer (Fig. S3). The α4 subunit also has an intra-subunit halothane site (#3) near the IC end of the TM domain. Halothane near the EC end of α4 (#4) more or less resided between intra- and inter-subunit site, where residues I268 and N221, L222 of α4 and K260 and V262 of β2 line the cavity. It appears that #4 is open for halothane to sample both intra- and inter-subunit cavities. Another inter-subunit site for halothane (#5) is supported by I450 of β2 and L283 of α4, where saturation transfer was observed (Fig. S3).

Collectively, both α4 and β2 have intra-subunit binding sites for halothane. The intra-subunit sites near the EC end and the IC end are homologous to the anesthetic site identified in the X-ray structures of GLIC [32] and a neurosteroid photolabeling site in the 3 subunit of the $GABA_A$ receptor [16], respectively. In addition to the intra-subunit sites, our NMR data revealed existence of inter-subunit sites for anesthetic binding.

3.2 Ketamine interaction sites in the α4β2 nAChR

Compared to volatile anesthetics, such as halothane, the intravenous anesthetic ketamine inhibits the function of the α4β2 nAChR at a lower concentration [51]. We added only 80 μM ketamine to the α4(β2) or β2(α4) samples and observed notable changes in chemical shift for several residues in ^{1}H-^{15}N HSQC spectra (Fig. 3, Figs. S4 and S5). Severe overlapping of proton signals of ketamine and protein prevented a reliable result from saturation transfer difference experiments. Thus, the ketamine sites were determined based on chemical shift perturbation. Two ketamine-binding sites emerged when the ketamine-perturbed residues were mapped onto the NMR structure of α4β2 (Fig. 4). One is reminiscent of the intra-subunit halothane site near the EC end of TM in β2 (Fig. 2).

Another is located near the IC end of TM between β2 and α4, where ketamine contacts I287 of β2 and V234 of α4. Ketamine perturbation to these residues propagated to other more remote residues (V283 and K246) and caused changes in their chemical shifts.

3.3 Anesthetic binding altered dynamics of the α4β2 nAChR

Motional characteristics of proteins are often reflected in peak intensities of residues in the NMR spectra [36, 52]. Residues at the N- and C-termini as well as exposed loops experience fast motions (on the ps-ns timescale) and have higher signal intensities than residues on helices (Fig. S6). Conversely, residues in the TM helices have weak intensity or invisible signals due to restricted motion or broadening due to conformational-exchange on the μ-ms timescale [53].

Upon addition of anesthetics, changes in motion or conformational exchange for residues in α4β2 are evident in the NMR spectra. The most remarkable change is splitting of single peaks into double peaks (for example, V236 and L222 of α4; Fig. 5A). The visibly separated double peaks could result from either a decrease in the rate of conformational exchange or a shift in the conformational distribution [54]. In the first scenario, a single NMR signal was detected when the exchange rate between the two conformations was faster than the NMR detection time scale. The single peaks became double peaks when anesthetics slowed down the exchange rate. The observed double peaks of V253 and L222 belong to this scenario. For shifting conformation equilibria by anesthetics, V236 of α4 gave a good example. In the second scenario, V236 had two populations (75% vs. 25%) with distinct resonance frequencies in the absence of halothane. The major peak shifted and its peak intensity dropped in an anesthetic concentration dependent manner. Conversely, the minor peak had less change in chemical shift but its intensity increased so that the two conformations became almost equal populated in the presence of 2 mM halothane. Thus, anesthetics have either decreased conformational exchange rates or shifted conformation equilibria.

In addition to the change in peak splitting, we observed increased and decreased signal intensities for some residues. When we highlight these residues in the structures of α4 and β2 (Fig 5), several features become clear. Most residues in the vicinity of anesthetic binding sites experienced dynamic changes. However, dynamic changes induced by anesthetics could extend beyond the binding sites, such as the case of dynamical changes at the upper helical region of α4 when ketamine bound to the inter-subunit site close to the IC end of the TM domain. It is also noticeable that loop residues of fast motion and high NMR signal intensities are not affected by anesthetics, but residues at junctions of helices and loops (V262 and S271 of β2 and I267, I268, S277 of α4) are susceptible for dynamical modulation by anesthetics. This observation is consistent with a previous NMR study on another membrane protein [38].

4. Discussion

4.1 A common general-anesthetic binding site near the EC end of the TM domain

Both the inhalational anesthetic halothane and the intravenous anesthetic ketamine have multiple interaction sites in the TM domains of the α4β2 nAChR. This finding is in accord with previous computational predictions [55–59] and experimental observations [15, 18, 19, 60] on the α4β2 nAChR and its homologous proteins.

Among different sites, the intra-subunit binding site near the EC end of the TM domain (#1 in Fig. 2 and Fig. 4) has been most substantiated by experiments on several homologous proteins. Photo-affinity labeling of [^{14}C] halothane to the *Torpedo* nAChR was identified on residue δ-Y228 [19], which is homologous to Y212 of β2 lining #1 halothane site (Fig. 2).

Fluorescence quenching experiments suggested halothane binding to an equivalent site in GLIC [60]. Furthermore, crystal structures of GLIC in complex with the anesthetics desflurane and propofol revealed the intra-subunit anesthetic binding site [32] that is in remarkable agreement with our NMR identified site for halothane or ketamine in the β2 subunit (Fig. S7). It is intriguing to see that in the absence of the EC domain, the TM domain alone presents the same anesthetic binding site as those intact homologous proteins. It signifies that our NMR structures for the α4β2 TM domains [35] well represent the same domains in the intact protein. Halothane and ketamine have very different molecular volumes and shapes. Their binding to this upper part of the TM domain of the α4β2 nAChR not only further supports the notion that the site is a common site for anesthetic binding to pentameric ligand gated ion channels [32], but also demonstrates the flexibility of the cavity to accommodate different anesthetics.

4.2 Additional anesthetic binding sites

Inter-subunit halothane binding sites at the interface of α4 and β2 (#4 and #5 in Fig. 2) are almost at the same height as the intra-subunit halothane site at the upper part of the TM domain. Several residues lining these sites were implicated previously as anesthetic-labeling residues in homologous proteins. L283 at the inter-subunit halothane-binding site is homologous to A288 of the α1 glycine receptor, where the site for alcohol and anesthetic action was rationalized [14, 61]. Although the X-ray structures of GLIC bound with desflurane or propofol revealed only the intra-subunit anesthetic binding site, the study recognized the possibility of anesthetic migration from intra- into inter-subunit cavities [32]. The NMR identified halothane sites (#4 and #5) in Fig. 2 add compelling evidence for anesthetic binding to the inter-subunit cavities. Ketamine, however, did not appear in the inter-subunit cavities at the upper part of the TM domain. The larger size of ketamine may have prevented the molecule from occupying both intra- and inter-subunit cavities.

Another discrete set of intra- or inter-subunit cavities for anesthetic binding was found at the IC end of the TM domains. Halothane or ketamine binding to this region of the α4β2 nAChR was observed for the first time, but halothane binding to the homologous region in GLIC (W213 and W217) was detected previously using fluorescence quenching [60]. The region of the IC end of TM was also shown for cholesterol binding in the *Torpedo* nAChR [62]. Neurosteroids modulate $GABA_A$ receptors via binding to the TM domains of the receptors [12, 63]. A neurosteroid-binding site at the IC end of the TM domain was recently indentified [16], highlighting the importance of this region in drug binding and modulating channel functions.

It is worth noting that anesthetic binding is not restricted only to the TM domain. They may also occupy cavities in the EC domain in the intact proteins. A recent crystal structure of GLIC in complex with ketamine shows that ketamine binds to an inter-subunit cavity in the EC domain and the ketamine binding inhibits GLIC current [64]. For the α4β2 nAChR, without the presence of the extracellular domain, the channels formed by the TM domains exhibit spontaneous opening and closing [35]. How much anesthetics increase the probability of channel closing and which binding site plays the most critical role in channel inhibition need to be investigated in future studies.

4.3 Anesthetic effects on dynamics

Conformational changes in the TM domains of the α4β2 nAChR constitute different functional states of the ion channel. Even in the absence of the EC domains and without agonist binding, the TM domains of α4 and 2 could form Na^+-conducting channels spontaneously in lipid vesicles [35]. Our NMR data show that anesthetic sites at the EC end of the TM domains are virtually located behind the channel gate, while the sites at the IC

end of the TM domains are adjacent to the ion selectivity filter. Both locations are crucial to channel function [32, 65, 66]. Conformational changes in these regions can affect transitions between different states of ion conductivity through channels.

Anesthetic modulation on channel motion was evidenced by changes of NMR signal intensities upon adding anesthetics, as well as peak splitting of the α4 and β2 residues at the EC and IC ends of the TM domains. Although changes in peak intensities alone could not tell whether anesthetics made conformational exchanges slower or faster, peak splitting unambiguously indicated a decrease in the conformational exchange rate on a μs-ms timescale [53]. Anesthetic occupancy of the α4β2 cavities may have reduced the degrees of freedom of interacting side chains and the attached backbone atoms, consequently resulting in decrease of exchange rate. For the same reason, anesthetic binding stabilized the original sub-conformation, shifted the conformational equilibria, and changed the population distribution of different conformations. The same trend of decrease in conformational exchange rates caused by anesthetics was also observed on other proteins [38, 39]. The results support the notion that multiple conformers coexist dynamically in ion channel proteins and general anesthetics can shift the equilibrium among different conformation states [67].

It is also imperative to know that dynamics changes occurred not only to residues adjacent to anesthetics, but also to residues remote from the anesthetic binding sites. The observation is in accord with the consensus of allosteric mechanisms of signal transduction [68]. Propagation of local anesthetic perturbation to remote sites, especially to the junctions of helices and loops, can lead functional consequences. Although ketamine does not bind near I267, I268, and S277 of α4, the observed motion changes in these residues are likely to affect communication between the EC and TM domains in the agonist-elicited channel activations [69, 70].

5. Conclusions

The study, for the first time, revealed multiple anesthetic binding sites in the TM domains of the α4β2 nAChR. The identified intra-subunit halothane and ketamine sites near the EC end of the TM domains are reminiscent of the previously reported site on homologous proteins [19, 32], supporting the notion that the identified site is a common anesthetic site. The inter-subunit sites near the EC end of the TM domains were observed for halothane but not for ketamine, suggesting that anesthetics of small sizes can “travel” between intra- and inter-subunit sites. The sites near the IC end of the TM domains were least documented for anesthetic binding in the literature. The finding of halothane and ketamine on these sites certainly adds more weights to the region.

The study also provided compelling experimental evidence of anesthetic-induced changes in protein dynamics, especially near regions of the hydrophobic gate and ion selectivity filter that directly regulate functions of the channel. Motion is essential for functions, especially for proteins like the α4β2 nAChR. Our data demonstrated that anesthetics could shift equilibra of coexisting conformers and modify the motion on the μs-ms timescale, which is on the same timescale of channel functions. Thus, these dynamics changes will impart a functional consequence. Furthermore, our study demonstrated dynamics changes beyond the binding sites and allosteric modulation of anesthetics on protein dynamics, suggesting that anesthetic binding to a few sites could introduce disturbance to the coupled motion in the molecular machinery of the α4β2 nAChR and ultimately alter functions of these proteins.

Supplementary Material

Refer to Web version on PubMed Central for supplementary material.

Acknowledgments

The authors thank Professor Rieko Ishima for the valuable discussion of protein dynamics. This work was supported by grants from the National Institute of Health (R01GM56257 and R01GM66358 to P.T. and R37GM049202 to Y.X.).

References

1. Forman SA, Miller KW. Anesthetic sites and allosteric mechanisms of action on Cys-loop ligand-gated ion channels. Can J Anaesth. 2011; 58:191–205. [PubMed: 21213095]
2. Campagna JA, Miller KW, Forman SA. Mechanisms of actions of inhaled anesthetics. N Engl J Med. 2003; 348:2110–2124. [PubMed: 12761368]
3. Evers AS, Steinbach JH. Supersensitive sites in the central nervous system. Anesthetics block brain nicotinic receptors. Anesthesiology. 1997; 86:760–762. [PubMed: 9105218]
4. Picciotto MR, Zoli M, Lena C, Bessis A, Lallemand Y, Le Novere N, Vincent P, Pich EM, Brulet P, Changeux JP. Abnormal avoidance learning in mice lacking functional high-affinity nicotine receptor in the brain. Nature. 1995; 374:65–67. [PubMed: 7870173]
5. Marubio LM, del Mar Arroyo-Jimenez M, Cordero-Erausquin M, Lena C, Le Novere N, de Kerchove d'Exaerde A, Huchet M, Damaj MI, Changeux JP. Reduced antinociception in mice lacking neuronal nicotinic receptor subunits. Nature. 1999; 398:805–810. [PubMed: 10235262]
6. Xu W, Orr-Urtreger A, Nigro F, Gelber S, Sutcliffe CB, Armstrong D, Patrick JW, Role LW, Beaudet AL, De Biasi M. Multiorgan autonomic dysfunction in mice lacking the beta2 and the beta4 subunits of neuronal nicotinic acetylcholine receptors. J Neurosci. 1999; 19:9298–9305. [PubMed: 10531434]
7. Mori T, Zhao X, Zuo Y, Aistrup GL, Nishikawa K, Marszalec W, Yeh JZ, Narahashi T. Modulation of neuronal nicotinic acetylcholine receptors by halothane in rat cortical neurons. Mol Pharmacol. 2001; 59:732–743. [PubMed: 11259617]
8. Yamashita M, Mori T, Nagata K, Yeh JZ, Narahashi T. Isoflurane modulation of neuronal nicotinic acetylcholine receptors expressed in human embryonic kidney cells. Anesthesiology. 2005; 102:76–84. [PubMed: 15618790]
9. Flood P, Ramirez-Latorre J, Role L. Alpha 4 beta 2 neuronal nicotinic acetylcholine receptors in the central nervous system are inhibited by isoflurane and propofol, but alpha 7-type nicotinic acetylcholine receptors are unaffected. Anesthesiology. 1997; 86:859–865. [PubMed: 9105230]
10. Zwart R, Vijverberg HP. Four pharmacologically distinct subtypes of alpha4beta2 nicotinic acetylcholine receptor expressed in Xenopus laevis oocytes. Mol Pharmacol. 1998; 54:1124–1131. [PubMed: 9855643]
11. Nelson ME, Kuryatov A, Choi CH, Zhou Y, Lindstrom J. Alternate stoichiometries of alpha4beta2 nicotinic acetylcholine receptors. Mol Pharmacol. 2003; 63:332–341. [PubMed: 12527804]
12. Hosie AM, Wilkins ME, da Silva HM, Smart TG. Endogenous neurosteroids regulate GABAA receptors through two discrete transmembrane sites. Nature. 2006; 444:486–489. [PubMed: 17108970]
13. Yamakura T, Borghese C, Harris RA. A transmembrane site determines sensitivity of neuronal nicotinic acetylcholine receptors to general anesthetics. J Biol Chem. 2000; 275:40879–40886. [PubMed: 11020384]
14. Mihic SJ, Ye Q, Wick MJ, Koltchine VV, Krasowski MD, Finn SE, Mascia MP, Valenzuela CF, Hanson KK, Greenblatt EP, Harris RA, Harrison NL. Sites of alcohol and volatile anaesthetic action on GABA(A) and glycine receptors. Nature. 1997; 389:385–389. [PubMed: 9311780]
15. Chiara DC, Dostalova Z, Jayakar SS, Zhou X, Miller KW, Cohen JB. Mapping general anesthetic binding site(s) in human alpha1beta3 gamma-aminobutyric acid type A receptors with [(3)H]TDBzl-etomidate, a photoreactive etomidate analogue. Biochemistry. 2012; 51:836–847. [PubMed: 22243422]
16. Chen ZW, Manion B, Townsend RR, Covey DF, Reichert DE, Steinbach JH, Sieghart W, Fuchs K, Evers AS. Neurosteroid Analogue Photolabeling of a Site in the TM3 Domain of the beta3 Subunit of the GABAA Receptor. Mol Pharmacol. 2012

17. Cui T, Mowrey D, Bondarenko V, Tillman T, Ma D, Landrum E, Perez-Aguilar JM, He J, Wang W, Saven JG, Eckenhoff RG, Tang P, Xu Y. NMR structure and dynamics of a designed water-soluble transmembrane domain of nicotinic acetylcholine receptor. Biochim Biophys Acta. 2012; 1818:617–626. [PubMed: 22155685]
18. Chiara DC, Hong FH, Arevalo E, Husain SS, Miller KW, Forman SA, Cohen JB. Time-resolved photolabeling of the nicotinic acetylcholine receptor by [3H]azietomidate, an open-state inhibitor. Mol Pharmacol. 2009; 75:1084–1095. [PubMed: 19218367]
19. Chiara DC, Dangott LJ, Eckenhoff RG, Cohen JB. Identification of nicotinic acetylcholine receptor amino acids photolabeled by the volatile anesthetic halothane. Biochemistry. 2003; 42:13457–13467. [PubMed: 14621991]
20. Eckenhoff RG. An inhalational anesthetic binding domain in the nicotinic acetylcholine receptor. Proc Natl Acad Sci U S A. 1996; 93:2807–2810. [PubMed: 8610122]
21. Nirthanan S, Garcia G 3rd, Chiara DC, Husain SS, Cohen JB. Identification of binding sites in the nicotinic acetylcholine receptor for TDBzl-etomidate, a photoreactive positive allosteric effector. J Biol Chem. 2008; 283:22051–22062. [PubMed: 18524766]
22. Li GD, Chiara DC, Sawyer GW, Husain SS, Olsen RW, Cohen JB. Identification of a GABAA receptor anesthetic binding site at subunit interfaces by photolabeling with an etomidate analog. J Neurosci. 2006; 26:11599–11605. [PubMed: 17093081]
23. Eckenhoff RG, Xi J, Shimaoka M, Bhattacharji A, Covarrubias M, Dailey WP. Azi-isoflurane, a Photolabel Analog of the Commonly Used Inhaled General Anesthetic Isoflurane. ACS chemical neuroscience. 2010; 1:139–145. [PubMed: 20228895]
24. Hall MA, Xi J, Lor C, Dai S, Pearce R, Dailey WP, Eckenhoff RG. m-Azipropofol (AziPm) a photoactive analogue of the intravenous general anesthetic propofol. Journal of medicinal chemistry. 2010; 53:5667–5675. [PubMed: 20597506]
25. Stewart DS, Savechenkov PY, Dostalova Z, Chiara DC, Ge R, Raines DE, Cohen JB, Forman SA, Bruzik KS, Miller KW. p-(4-Azipentyl)propofol: a potent photoreactive general anesthetic derivative of propofol. Journal of medicinal chemistry. 2011; 54:8124–8135. [PubMed: 22029276]
26. Hilf RJ, Dutzler R. X-ray structure of a prokaryotic pentameric ligand-gated ion channel. Nature. 2008; 452:375–379. [PubMed: 18322461]
27. Hilf RJ, Dutzler R. Structure of a potentially open state of a proton-activated pentameric ligand-gated ion channel. Nature. 2009; 457:115–118. [PubMed: 18987630]
28. Bocquet N, Nury H, Baaden M, Le Poupon C, Changeux JP, Delarue M, Corringer PJ. X-ray structure of a pentameric ligand-gated ion channel in an apparently open conformation. Nature. 2009; 457:111–114. [PubMed: 18987633]
29. Hibbs RE, Gouaux E. Principles of activation and permeation in an anion-selective Cys-loop receptor. Nature. 2011; 474:54–60. [PubMed: 21572436]
30. Pan J, Chen Q, Willenbring D, Yoshida K, Tillman T, Kashlan OB, Cohen A, Kong XP, Xu Y, Tang P. Structure of the pentameric ligand-gated ion channel ELIC cocrystallized with its competitive antagonist acetylcholine. Nature communications. 2012; 3:714.
31. Hilf RJ, Bertozzi C, Zimmermann I, Reiter A, Trauner D, Dutzler R. Structural basis of open channel block in a prokaryotic pentameric ligand-gated ion channel. Nature structural & molecular biology. 2010; 17:1330–1336.
32. Nury H, Van Renterghem C, Weng Y, Tran A, Baaden M, Dufresne V, Changeux JP, Sonner JM, Delarue M, Corringer PJ. X-ray structures of general anaesthetics bound to a pentameric ligand-gated ion channel. Nature. 2011; 469:428–431. [PubMed: 21248852]
33. Tang P, Mandal PK, Xu Y. NMR structures of the second transmembrane domain of the human glycine receptor alpha(1) subunit: model of pore architecture and channel gating. Biophys J. 2002; 83:252–262. [PubMed: 12080117]
34. Kandasamy SK, Lee DK, Nanga RP, Xu J, Santos JS, Larson RG, Ramamoorthy A. Solid-state NMR and molecular dynamics simulations reveal the oligomeric ion-channels of TM2-GABA(A) stabilized by intermolecular hydrogen bonding. Biochim Biophys Acta. 2009; 1788:686–695. [PubMed: 19071084]
35. Bondarenko V, Mowrey D, Tillman T, Cui T, Liu LT, Xu Y, Tang P. NMR structures of the transmembrane domains of the alpha4beta2 nAChR. Biochim Biophys Acta. 2012

36. Bondarenko V, Tillman T, Xu Y, Tang P. NMR structure of the transmembrane domain of the n-acetylcholine receptor beta2 subunit. Biochim Biophys Acta. 2010; 1798:1608–1614. [PubMed: 20441771]

37. Cui T, Canlas CG, Xu Y, Tang P. Anesthetic effects on the structure and dynamics of the second transmembrane domains of nAChR alpha4beta2. Biochim Biophys Acta. 2010; 1798:161–166. [PubMed: 19715664]

38. Canlas CG, Cui T, Li L, Xu Y, Tang P. Anesthetic modulation of protein dynamics: insight from an NMR study. J Phys Chem B. 2008; 112:14312–14318. [PubMed: 18821786]

39. Cui T, Bondarenko V, Ma D, Canlas C, Brandon NR, Johansson JS, Xu Y, Tang P. Four-alpha-helix bundle with designed anesthetic binding pockets. Part II: halothane effects on structure and dynamics. Biophys J. 2008; 94:4464–4472. [PubMed: 18310239]

40. Bondarenko V, Yushmanov VE, Xu Y, Tang P. NMR study of general anesthetic interaction with nAChR beta2 subunit. Biophys J. 2008; 94:1681–1688. [PubMed: 17993502]

41. Tang P, Eckenhoff RG, Xu Y. General anesthetic binding to gramicidin A: the structural requirements. Biophys J. 2000; 78:1804–1809. [PubMed: 10733961]

42. Xu Y, Seto T, Tang P, Firestone L. NMR study of volatile anesthetic binding to nicotinic acetylcholine receptors. Biophys J. 2000; 78:746–751. [PubMed: 10653787]

43. Tang P, Hu J, Liachenko S, Xu Y. Distinctly different interactions of anesthetic and nonimmobilizer with transmembrane channel peptides. Biophys J. 1999; 77:739–746. [PubMed: 10423422]

44. Mayer M, Meyer B. Characterization of ligand binding by saturation transfer difference NMR spectroscopy. Angewandte Chemie-International Edition. 1999; 38:1784–1788.

45. Wishart DS, Bigam CG, Yao J, Abildgaard F, Dyson HJ, Oldfield E, Markley JL, Sykes BD. 1H, 13C and 15N chemical shift referencing in biomolecular NMR. J Biomol NMR. 1995; 6:135–140. [PubMed: 8589602]

46. Delaglio F, Grzesiek S, Vuister GW, Zhu G, Pfeifer J, Bax A. NMRPipe: a multidimensional spectral processing system based on UNIX pipes. J Biomol NMR. 1995; 6:277–293. [PubMed: 8520220]

47. Goddard, TD.; Kneller, DG. SPARKY. Vol. 3. University of California; San Francisco: 2001.

48. Morris GM, Goodsell DS, Halliday RS, Huey R, Hart WE, Belew RK, Olson AJ. Automated docking using a Lamarckian genetic algorithm and an empirical binding free energy function. Journal of Computational Chemistry. 1998; 19:1639–1662.

49. Takahashi H, Nakanishi T, Kami K, Arata Y, Shimada I. A novel NMR method for determining the interfaces of large protein-protein complexes. Nat Struct Biol. 2000; 7:220–223. [PubMed: 10700281]

50. Ramos A, Kelly G, Hollingworth D, Pastore A, Frenkiel T. Mapping the interfaces of protein-nucleic acid complexes using cross-saturation. Journal of the American Chemical Society. 2000; 122:11311–11314.

51. Coates KM, Flood P. Ketamine and its preservative, benzethonium chloride, both inhibit human recombinant alpha7 and alpha4beta2 neuronal nicotinic acetylcholine receptors in Xenopus oocytes. Br J Pharmacol. 2001; 134:871–879. [PubMed: 11606328]

52. Frueh DP, Arthanari H, Koglin A, Vosburg DA, Bennett AE, Walsh CT, Wagner G. Dynamic thiolation-thioesterase structure of a non-ribosomal peptide synthetase. Nature. 2008; 454:903–906. [PubMed: 18704088]

53. Rao BD. Nuclear magnetic resonance line-shape analysis and determination of exchange rates. Methods Enzymol. 1989; 176:279–311. [PubMed: 2811690]

54. Ishima R, Torchia DA. Protein dynamics from NMR. Nat Struct Biol. 2000; 7:740–743. [PubMed: 10966641]

55. Liu LT, Willenbring D, Xu Y, Tang P. General anesthetic binding to neuronal alpha4beta2 nicotinic acetylcholine receptor and its effects on global dynamics. J Phys Chem B. 2009; 113:12581–12589. [PubMed: 19697903]

56. Liu LT, Haddadian EJ, Willenbring D, Xu Y, Tang P. Higher susceptibility to halothane modulation in open- than in closed-channel alpha4beta2 nAChR revealed by molecular dynamics simulations. J Phys Chem B. 2010; 114:626–632. [PubMed: 20014754]

57. Mowrey D, Haddadian EJ, Liu LT, Willenbring D, Xu Y, Tang P. Unresponsive correlated motion in alpha7 nAChR to halothane binding explains its functional insensitivity to volatile anesthetics. J Phys Chem B. 2010; 114:7649–7655. [PubMed: 20465243]
58. Brannigan G, LeBard DN, Henin J, Eckenhoff RG, Klein ML. Multiple binding sites for the general anesthetic isoflurane identified in the nicotinic acetylcholine receptor transmembrane domain. Proc Natl Acad Sci U S A. 2010; 107:14122–14127. [PubMed: 20660787]
59. Willenbring D, Liu LT, Mowrey D, Xu Y, Tang P. Isoflurane alters the structure and dynamics of GLIC. Biophys J. 2011; 101:1905–1912. [PubMed: 22004744]
60. Chen Q, Cheng MH, Xu Y, Tang P. Anesthetic binding in a pentameric ligand-gated ion channel: GLIC. Biophys J. 2010; 99:1801–1809. [PubMed: 20858424]
61. Murail S, Wallner B, Trudell JR, Bertaccini E, Lindahl E. Microsecond simulations indicate that ethanol binds between subunits and could stabilize an open-state model of a glycine receptor. Biophys J. 2011; 100:1642–1650. [PubMed: 21463577]
62. Hamouda AK, Chiara DC, Sauls D, Cohen JB, Blanton MP. Cholesterol interacts with transmembrane alpha-helices M1, M3, and M4 of the Torpedo nicotinic acetylcholine receptor: photolabeling studies using [3H] Azicholesterol. Biochemistry. 2006; 45:976–986. [PubMed: 16411773]
63. Hosie AM, Clarke L, da Silva H, Smart TG. Conserved site for neurosteroid modulation of GABA A receptors. Neuropharmacology. 2009; 56:149–154. [PubMed: 18762201]
64. Pan J, Chen Q, Willenbring D, Mowrey D, Kong X-P, Cohen A, Divito CB, Xu Y, Tang P. Structure of the pentameric ligand-gated ion channel GLIC bound with anesthetic ketamine. Structure. 2012; 20:1463–1469. [PubMed: 22958642]
65. Corringer PJ, Bertrand S, Galzi JL, Devillers-Thiery A, Changeux JP, Bertrand D. Mutational analysis of the charge selectivity filter of the alpha7 nicotinic acetylcholine receptor. Neuron. 1999; 22:831–843. [PubMed: 10230802]
66. Cymes GD, Grosman C. Tunable pKa values and the basis of opposite charge selectivities in nicotinic-type receptors. Nature. 2011; 474:526–530. [PubMed: 21602825]
67. Tang P, Xu Y. Large-scale molecular dynamics simulations of general anesthetic effects on the ion channel in the fully hydrated membrane: the implication of molecular mechanisms of general anesthesia. Proc Natl Acad Sci U S A. 2002; 99:16035–16040. [PubMed: 12438684]
68. Changeux JP, Edelstein SJ. Allosteric mechanisms of signal transduction. Science. 2005; 308:1424–1428. [PubMed: 15933191]
69. Szarecka A, Xu Y, Tang P. Dynamics of heteropentameric nicotinic acetylcholine receptor: implications of the gating mechanism. Proteins. 2007; 68:948–960. [PubMed: 17546671]
70. Lee WY, Free CR, Sine SM. Binding to gating transduction in nicotinic receptors: Cys-loop energetically couples to pre-M1 and M2-M3 regions. J Neurosci. 2009; 29:3189–3199. [PubMed: 19279256]

Highlights

- Anesthetics halothane and ketamine bound to multiple sites of the α4β2 nAChR
- A common intra-subunit anesthetic site was near the extracellular end of the β2 TM
- Halothane occupied inter-subunit sites near the extracellular end of the TM domain
- Both drugs bound to intra- and inter-subunit sites near the selectivity filter
- Anesthetics induced, directly or allosterically, dynamics changes of α4β2

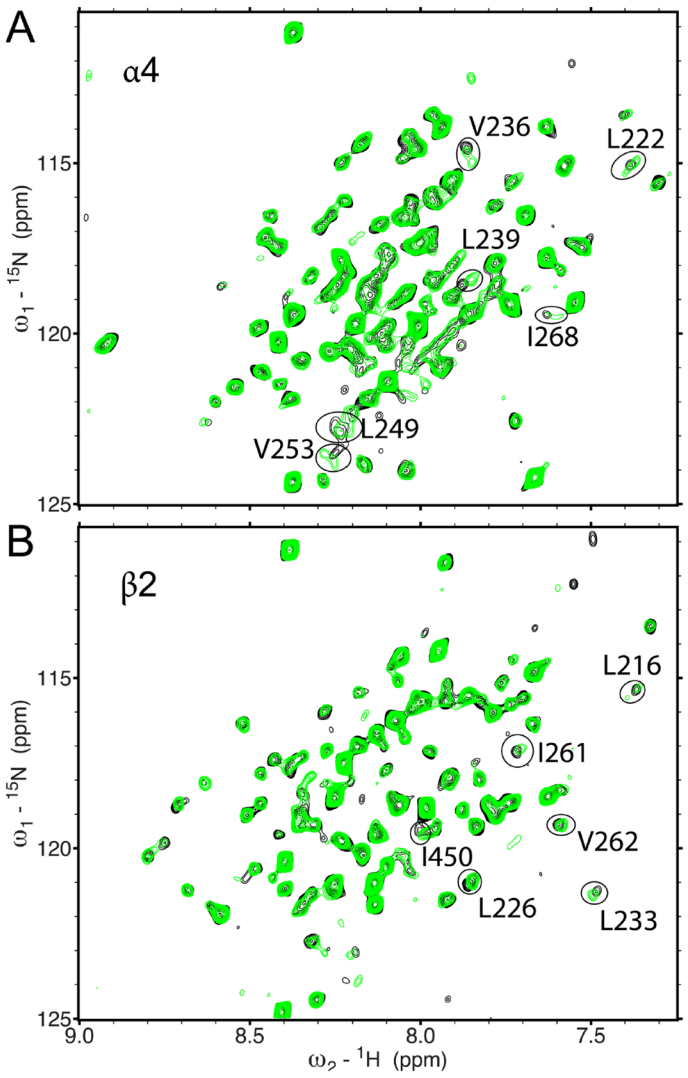

Fig. 1.

Residues involved in halothane binding using ^{1}H-^{15}N TROSY-HSQC spectra of the transmembrane domain of the human α4β2 n-acetylcholine receptor in the absence (black) and presence (green) of 2 mM halothane. (**A**) α4(β2), where only α4 is ^{15}N-labeled; (**B**) β2(α4), where only β2 is ^{15}N-labeled. For clarity, the chemical shift assignment for each peak is omitted here but provided in the Supplementary Material (Figs. S1 and S2). Peaks displaying significant changes in chemical shift are circled.

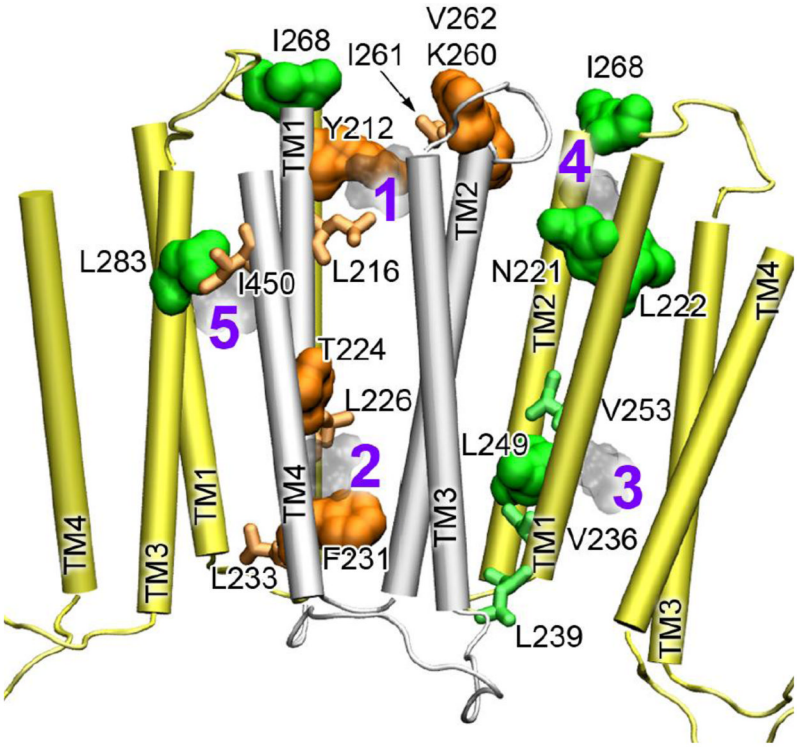

Fig. 2.

Multiple halothane-binding sites in the α4β2 nAChR. The TM domains of α4 and 2 are colored in yellow and silver, respectively. Residues of α4 (green) and β2 (orange) are highlighted in the surface presentation if they show direct interactions with halothane in the 2D saturation transfer experiments or in the stick presentation if they show changes in chemical shift upon halothane binding. The docked halothane molecules are numbered and shown in light gray. Note the inter-subunit sites, #4 and #5.

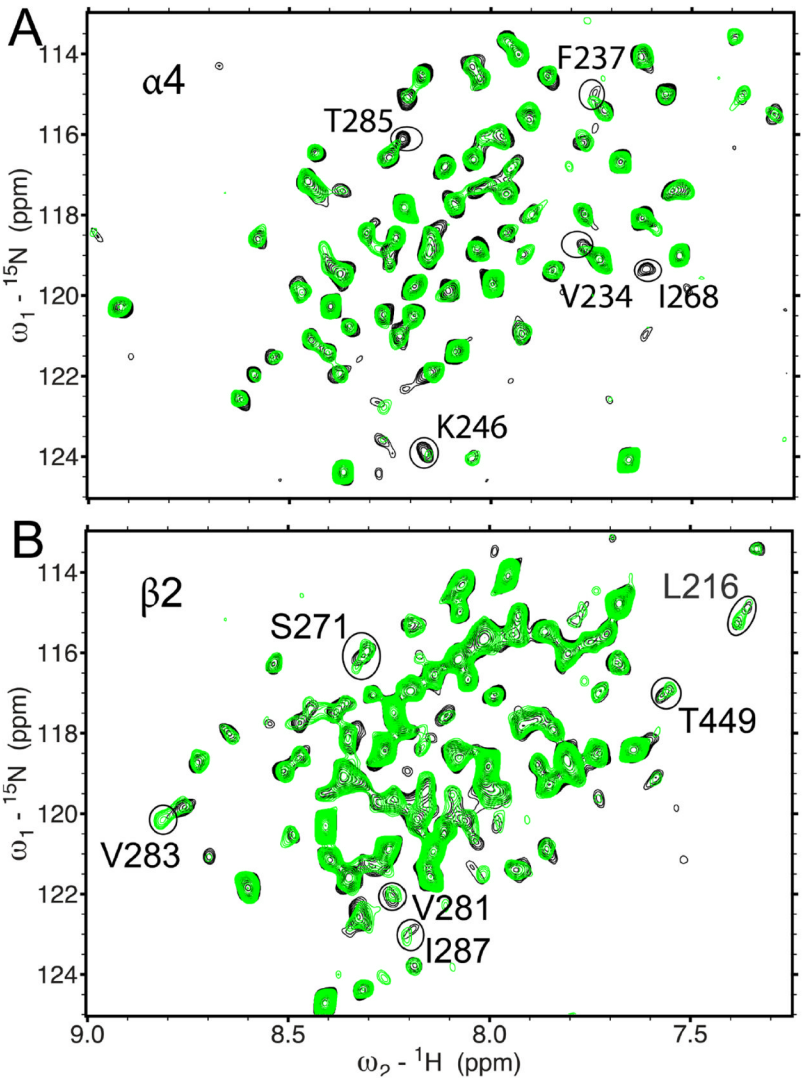

Fig. 3.

Residues involved in ketamine binding using ^{1}H-^{15}N TROSY-HSQC spectra of the transmembrane domain of the human α4β2 n-acetylcholine receptor in the absence (black) and presence (green) of 80 μM ketamine. (**A**) α4(β2), where only α4 is ^{15}N-labeled; (**B**) β2(α4), where only β2 is ^{15}N-labeled. For clarity, the chemical shift assignment for each peak is omitted here but provided in the Supplementary Material (Figs. S4 and S5). Peaks displaying significant changes in chemical shift are circled.

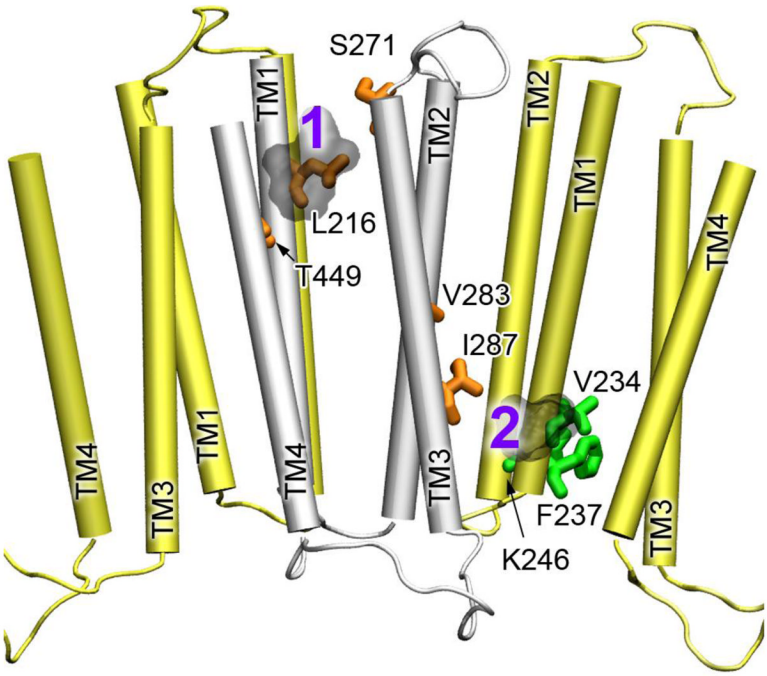

Fig. 4.

The ketamine-binding sites in the α4β2 nAChR. The TM domains of α4 and 2 are colored in yellow and silver, respectively. The residues of α4 and β2 showing changes in chemical shift upon halothane binding are highlighted in green and orange sticks, respectively. The docked ketamine molecules are numbered and shown in light gray.

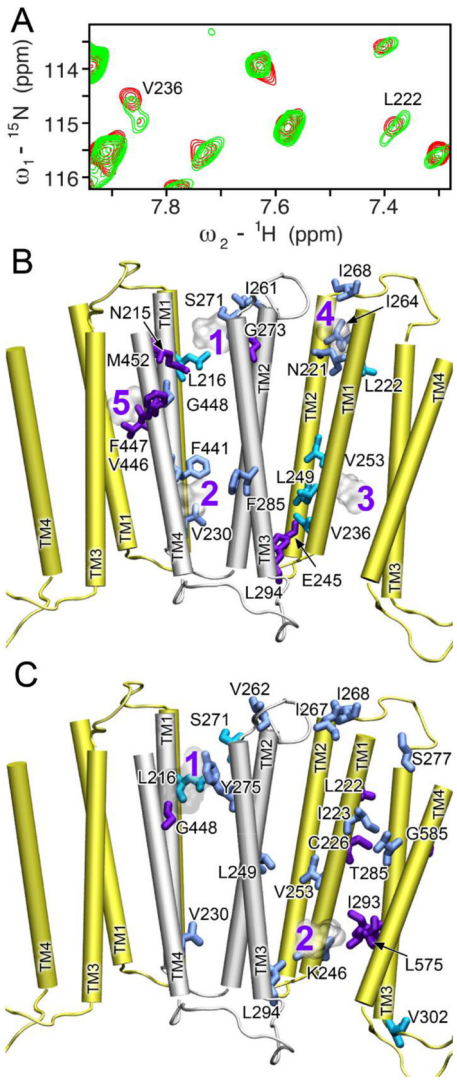

Fig. 5.

Anesthetics changed dynamics of residues in the α4β2 TM domains. (**A**) A representative expanded region of the ^{1}H-^{15}N TROSY-HSQC spectra for α4(β2) in the absence (black) and presence (red) of 2 mM halothane. Note the peak splitting for L222 and V236, indicative of slow exchange. (**B**) Residues experienced dynamics changes upon halothane binding are highlighted on the α4 (yellow) and β2 (silver) structures. (**C**) Residues experienced dynamics changes upon ketamine binding are highlighted on the α4 (yellow) and β2 (silver) structures. Three scenarios of dynamics changes are included in both (B) and (C): residues exhibiting peak splitting (cyan), decreases in peak intensity (blue), and increases in peak intensity (purple). Halothane and ketamine are shown in ghost representation to assist viewing each binding site.